17th World Conference on Earthquake Engineering, 17WCEE
Sendai, Japan - September 13th to 18th 2020

FINITE ELEMENT ANALYSIS OF RUBBER BEARINGS WITH LOW SHAPE FACTOR UNDER SEISMC EXCITATION

A. Orfeo[(1)], E. Tubaldi[(2)], A. Muhr[(3)], D. Losanno [(4)]

[(1)] *PhD, Department of Civil and Environmental Engineering, University of Strathclyde, Glasgow, UK, alessandra.orfeo@strath.ac.uk*
[(2)] *Lecturer, Department of Civil and Environmental Engineering, University of Strathclyde, Glasgow, UK, enrico.tubaldi@strath.ac.uk*
[(3)] *Researcher, Tun Abdul Razak Research Centre-TARRC, Hertford SG13 8NL, UK, amuhr@tarrc.co.uk*
[(4)] *Researcher, Construction Technologies Institute, National Research Council of Italy, San Giuliano Milanese, Milano, Italy, losanno@itc.cnr.it.*

Abstract

Keywords: isolation system, low shape factor rubber bearing, FE simulations, hyperelastic material, seismic response

Laminated elastomeric bearings are frequently employed to protect from the damaging effects of earthquakes critical facilities, such as nuclear power plants or hospital buildings and health care facilities. The bearings used in these applications are usually expensive, large and heavy. The high cost of conventional laminated bearings is attributed to the labor involved in steel plate and rubber sheets assembling, with the steel plates that need to be bonded to the rubber layers via a vulcanization process, and the cost of materials: high quality natural rubber, steel and bonding agent. One way to reduce the cost of laminated bearings and increase their use for seismic isolation is by minimizing the number of reinforced steel plates, which are used to provide vertical stiffness to the isolators, thus resulting in low values of the shape factor. Bearings with low shape factors have a lower vertical stiffness than traditional ones, but they can be effective in three-dimensional isolation, as they can be subjected to relatively large compressions and rotations. An accurate level of modelling of the behavior of these devices is of great importance, as the integrity of isolated structures relies heavily on their response. Based on a previous experimental campaign on a prototype isolated building carried out at TARRC and University of Naples, this work illustrates the development of a finite element (FE) modeling strategy for describing the mechanical behavior of low-shape factor rubber bearings, and the seismic response of buildings isolated with them. The numerical research, conducted with Abaqus, consists of two parts, one simulating material and bearing tests, and the second one shaking table tests of an isolated prototype. In the first part of the study, an hyperelastic material model is calibrated based on the results of double-shear material tests, and a quasi-static analysis is performed on the bearing model, by imposing increasing shear deflections under a constant vertical compression. The obtained shear-deflection response is compared with experimental results to validate the developed model. In the second part of the study, the response of the isolated structure under seismic excitation is carried out, combining a three-dimensional modeling approach for the bearings with a description of the superstructure based on beam elements. An implicit dynamic analysis is performed, by monitoring the top acceleration, the interstorey drift and isolator relative displacement response under the earthquake record. The analysis results are compared with those measured from the shaking table test. The good agreement between the model prediction and experimental data provides strong support for the developed FE model and the assumed laws describing the rubber material behavior. The proposed modeling strategy will be used in future studies to investigate the response under a wide range of seismic input and to calibrate simplified approaches for simulating the coupled horizontal-vertical response of the bearings.

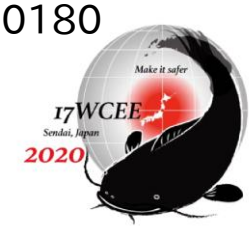

1. Introduction

Seismic isolation is an earthquake-resistant design strategy aimed at shifting the fundamental frequency of structures away from the predominant frequencies of the earthquake ground motion. Laminated rubber bearings are among the most widely used type of isolation system. They consist of multiple layers of rubber vulcanized to steel reinforcing layers that produce a vertically stiff but horizontally flexible isolator [1]. A non-dimensional parameter usually employed to characterize the geometry of these bearing is the primary shape factor, S1. This defines the ratio of the loaded area to the area free to bulge for an individual rubber layer [2, 3]. Common values of S1 are in the order of 10-20. This is to enhance the critical load capacity of the bearings and to minimise rocking motion in isolated structures by providing a large vertical stiffness while maintaining a low horizontal stiffness. However, high S1 values result in significant weight of the bearings, a large number of steel plates, and thus generally high production and installation costs. At the same time, the high vertical stiffness of the bearings yields very low periods of vibration of the isolated structure in the vertical direction. This could be a problem for critical facilities, such as nuclear power plants or hospitals, where it is necessary to provide effectively protection to sensitive equipment from the vertical component of earthquake ground motion. Moreover, the benefit of suppression of rocking is not entirely self-evident. For example, a fundamental response mode is lowered in the frequency if the vertical stiffness of the bearings is reduced, for a given lateral stiffness, thus shifting further away the system from resonance with the horizontal ground motion input. Also, vertical deflection of the bearings enhances their stability by strongly increasing the tangent tilting stiffness of the individual bonded sandwiches.

Since the early stages of development of seismic isolation bearings, researchers have investigated the possibility of employing low shape factor (LSF) rubber bearings as a way to achieve an economic 3D isolation of structural systems. It is noteworthy that the first example of structure isolated using rubber bearings, the Pestalozzi school built in 1969 in Skopje, Macedonia, was realized using completely unreinforced rubber blocks, causing a significant lateral bulging due to the weight of the building. A base-isolated laboratory building realized in Kajima Corporation Technical Research Institute [4] was one of the earliest applications that considered the use of low shape factor bearings. The two-story reinforced concrete building was supported on eighteen bearings with steel bars to provide damping. The aim was to provide 3D seismic isolation from earthquake as well as ambient ground vibrations and the effectiveness of the system has been showed in the laboratory testing. Aiken et al. [5] designed a 3D isolation system for a liquid metal reactor building. The study involved the design and testing of LSF bearings made from different types of rubber material and the analytical model for the behaviour of seismic isolation bearings. However, the dynamic response of the structure supported on such bearings was not experimentally investigated. Cilento et al. [6] carried out an extensive experimental campaign to analyse the behaviour of a prototype building isolated with natural rubber bearing with S1=1.32. The experimental campaign included also tests carried out at material and bearing level, as well as shaking table tests, demonstrating the effectiveness of isolating a structure with very low shape factor bearings. Warn [7] performed an analytical study, showing how buildings isolated on low shape factor bearings could experience minor non-structural damage following a major earthquake event.

Bearings with low shape factors are characterized by a significant coupling between the horizontal and vertical response. In particular, vertical loads induce a significant reduction of the horizontal stiffness. Moreover, the vertical pressure influences the damping capabilities under horizontal loading. To provide a simple interpretation of these aspects, a simple mechanical model was developed in the past by Koh and Kelly [8, 9], which was validated via some experimental results. However, this theory was validated by considering bearings with relatively high shape factor values and it fails in providing a description of the behaviour of low shape factor bearings. For example, the bearing investigated in Cilento et al. [6], subjected to axial load levels exceeding by two times the theoretical critical load, did not buckle and showed a stable behaviour under horizontal loading. This motivates the need for carrying out further experimental and numerical studies on LSF bearings.

This paper aims to further explore the LSF concept in rubber bearings through the development of a finite element (FE) modelling strategy for modelling these isolation devices. This strategy can be used 1) to achieve a deeper understanding of the mechanical behaviour of LSF bearing under combined axial and horizontal loads, 2) to numerically investigate the dynamic behaviour of systems isolated with the devices, and 3) to develop and validate simplified modelling approaches such as those proposed by Muhr [10]. The proposed modelling strategy is calibrated and validated based on the results of the experimental campaign carried out by Tun Abdul Razak Research Center (TARRC) rubber research centre and University of Naples Federico II on a structural prototype with LSF rubber bearings made with lightly filled natural rubber [6]. First, double shear tests results are used to calibrate the parameters of the hyperealstic constitutive materials used for describing the rubber layers. Subsequently, the quasi-static tests carried out on the bearings under constant vertical loads and cyclic horizontal displacement amplitudes are simulated. Finally, comparisons are made between the response of an isolated steel frame prototype with LSF bearings evaluated experimentally in a shaking table tests and the response obtained by using the 3D numerical model.

2. Material and bearing tests

2.1 Description of tests

Different mixes of natural rubber were used for manufacturing the bearings, which were characterized by different level of damping capacity. In this work the focus is on the lightly filled natural rubber compound (Mix 1 in [6]). The material dynamic behaviour was characterized by means of double shear displacement-controlled tests under sinusoidal input at different amplitude values, as described in [6]. The samples considered (see Fig. 1a) consist of two rubber cylinders connected through metal pieces. The thickness of the samples is 6mm and the diameter is 25mm. Using the data from the double-shear test on rubber, shear stiffness is defined as the ratio between the maximum shear force and the maximum displacement. According to the secant method, shear modulus G is defined as the ratio between the maximum shear stress τ (obtained by dividing the maximum shear force by the cross-sectional area of the rubber sample) and the maximum average shear strain γ, defined as the ratio between the shear displacement and the total rubber height. The results show that the lightly filled natural rubber has a shear modulus that changes slightly with the shear strain (Fig. 1b).

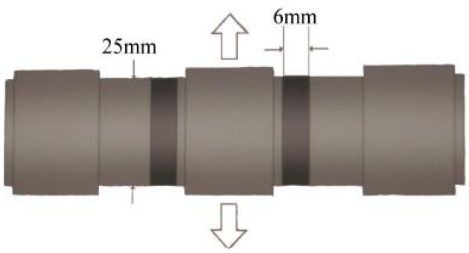

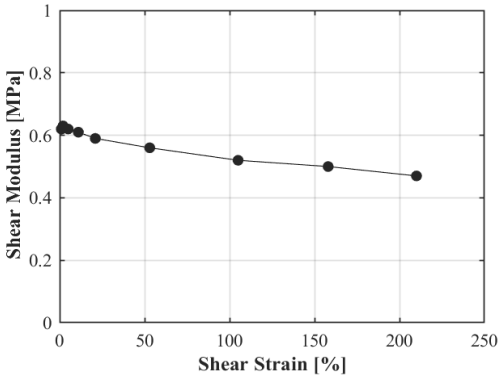

(a) (b)

Fig. 1 – (a) Double shear test piece geometry, (b) Shear modulus-shear strain relation

Fig. 2a illustrates the bearings considered in the tests. These bearings consist of three layers of rubber 19mm thick, two steel plates 4mm thick between the rubber layers and two steel end plates 2mm thick, designed to achieve a shape factor SF=1.32. The bearings are completed with steel end plates 130 mm x100 mm, with thickness 10mm. Four bearings were built and tested at TARRC and each pair of bearings was subjected to

dynamic shear and static compression loading simultaneously in a double shear configuration. A hydraulic jack was used to apply a compression force to the bearings to simulate gravity loads, whereas the shear displacements were imposed by a Dartec uniaxial servohydraulic actuator. The testing sequence consisted of two cycles of sinusoidal displacement at increasing shear strain amplitudes [6]. Shear stiffness is calculated from the hysteresis loops obtained from the shear tests, and was defined based on values of peak force F_{max} and peak displacement d_{max}:

$$k_s = F_{\max} / d_{\max} \tag{1}$$

Fig. 2b shows the shear stiffness values of one bearing for increasing shear strains, under a constant axial load of 19kN.

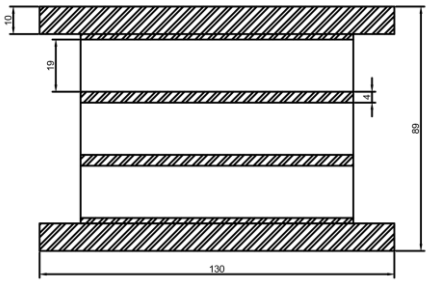

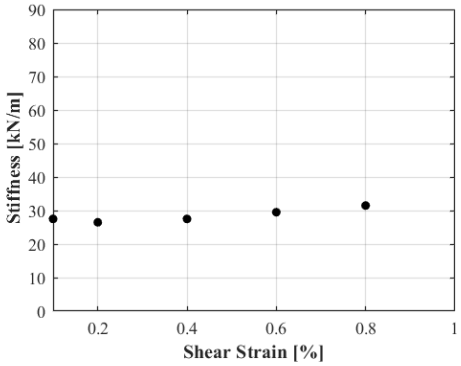

(a) (b)

Fig. 2 – (a) Bearing geometry, (b) Shear stiffness vs. average shear strain of a bearing from double shear test.

2.3 Numerical model

This subsection describes the numerical models of the double shear test-pieces and of the three-dimensional elastomeric bearings developed in Abaqus [11]. The Ogden hyperelastic material model is used for describing the elastomeric material behaviour. Assuming that the rubber is incompressible, the material strain energy function W depends on the three principal stretches $\lambda_1, \lambda_2, \lambda_3$ and $2N$ material constants, i.e. the hyperelastic parameters, μ_i and α_i , according to the following expression:

$$W = \sum_{i=1}^{N} \frac{\mu_i}{\alpha_i} \left(\lambda_1^{\alpha_i} + \lambda_2^{\alpha_i} + \lambda_3^{\alpha_i} - 3 \right) \tag{2}$$

where N is the number of polynomials that constitute the strain energy density function. The values of μ_i and α_i appearing in the Eq. (2) can be obtained from the double shear experiments described in the previous section. The definition of a hyperelastic material model in Abaqus [11] requires as input the uniaxial (or biaxial/triaxial) stress-strain data. Thus, the shear stress-strain data from the experiments need to be converted into an equivalent uniaxial one. The equivalence is based on the first strain invariant, which in the case of shear deformation is equal to $I_1 = I_2 = \gamma^2 + 3$, where γ is the shear strain. It is noteworthy that the Cauchy stresses (representing the forces over area in the deformed configuration) can be derived by differentiating the strain energy density function W as follows:

$$\boldsymbol{\sigma} = \frac{2}{J} \cdot \mathbf{B} \cdot \frac{\partial W}{\partial \mathbf{B}} = \frac{1}{J} \cdot \frac{\partial W}{\partial \mathbf{B}} \cdot \mathbf{F}^T \tag{3}$$

Where $\mathbf{B} = \mathbf{F} \cdot \mathbf{F}^T$ is the left Cauchy-Green strain tensor, $\mathbf{F}$ is the strain gradient tensor and $J = \det(\mathbf{F})$.

Fig. 3 describes the FE model of the double shear test. Since the double shear configuration has a plane of symmetry, only half of a layer is modelled, in order to reduce the computational cost of the simulation, by imposing appropriate boundary conditions. In all bearing models, the rubber components are modelled using 8-node solid elements (C3D8H) with first-order hybrid formulation, which is recommended for incompressible materials [12]. The mesh size is optimized to guarantee accurate results. In the simulation, a sinusoidal load in the horizontal direction is applied to the top reference point through displacement control and the bottom of the layer was fixed.

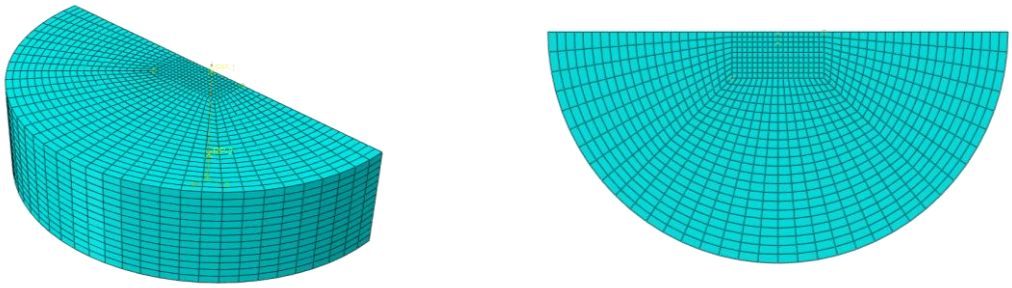

(a) (b)

Fig. 3 – FE model and meshing of the double shear test (a) 3D Perspective, (b) Top View.

Fig. 4a shows a vertical section along the diameter of the reference cylindrical layer under a shear displacement of 6 mm. This corresponds to an average shear strain of 100%. The local shear strains in the rubber are quite uniform and their value is very close to the average shear strain. Based on the hysteresis loop shown in Fig. 4b it is observed that the reference material model reproduces accurately the shear force-shear displacement diagram of the available experimental results. Table 1 reports and compares the shear stiffness values from both the experimental tests and the FE analysis results for a shear strain 105%. A good agreement between simulation and the test is found at this strain amplitude and also at lower ones.

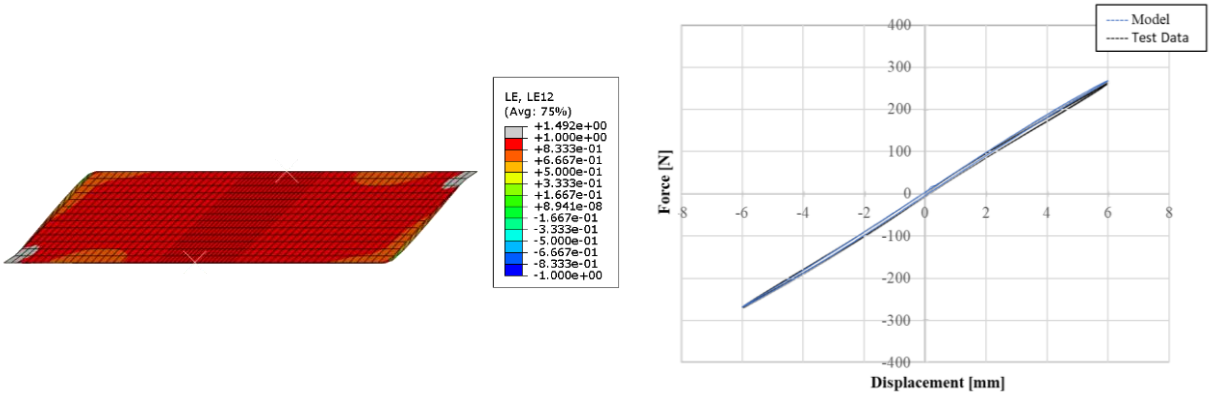

(a) (b)

Fig. 4 – (a) Contour plot of the shear strain component within the rubber testpiece, (b) Hysteresis loop of each rubber testpiece for an average maximum shear strain of 100%

Fig. 5 illustrates the model of the bearing, which is the same as those employed in the shaking table test, whose results are discussed in the next section. The intermediate steel shim plates and end plates are also modelled using C3D8H elements. The tie contact between steel and rubber layers of the bearing is expressed by contact pair option available in Abaqus [11]. The bottom anchor plate is fixed in all degrees of freedom and the top end plate is fixed against rotation but allowed to translate laterally and vertically.

Table 1 Experimental and numerical values of shear stiffness at shear strain 105%

Experiment		FE Modeling	
Average shear strain	Shear Stiffness (kN/m)	**Average shear strain**	Shear Stiffness (kN/m)
105 %	43.97	**105 %**	44.51

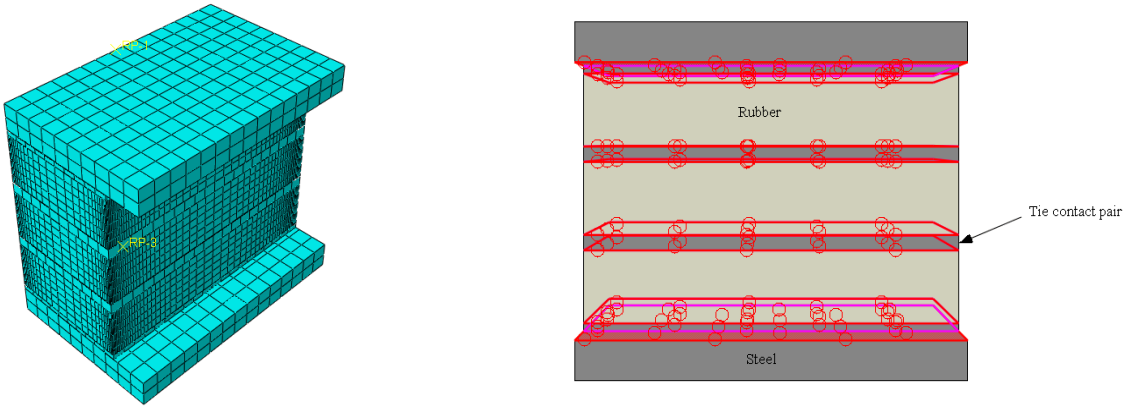

(a) (b)

Fig. 5 – Elastomeric Bearing: (a) Meshing, (b) Details of connections between various layers.

A vertical downward displacement is first imposed at the top plate, until a compressive load of 19kN is achieved. This value is the same as the one observed in the bearings under the gravity loads in the shaking table tests. Subsequently, two cycles of sinusoidal displacements are applied while preventing vertical motion and rotation of the top plate. Fig. 6a illustrates the deformed shape of the bearing subjected to horizontal displacement of 45.6 mm, i.e. an average shear strain of 80%.

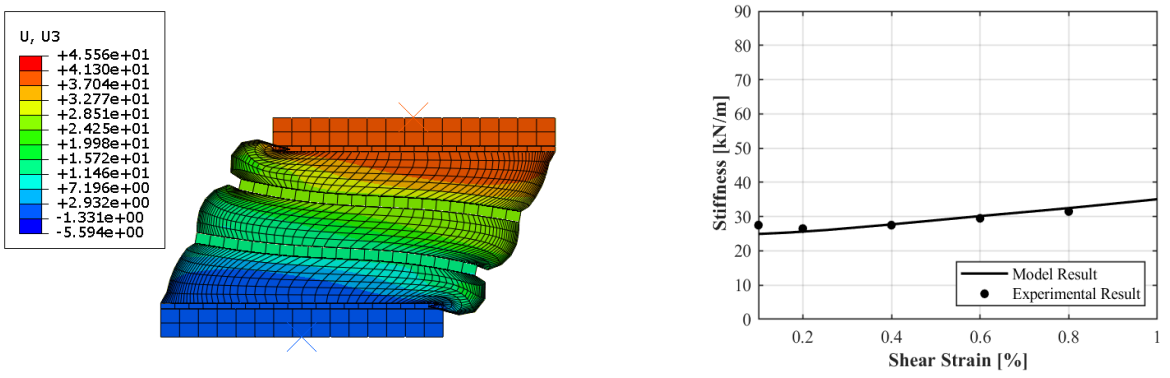

(a) (b)

Fig. 6 – (a) Horizontal displacement of the bearing for compressive load 19kN and shear strain 80%, (b) shear stiffness- average shear strain relation

The horizontal secant stiffness of the bearing, computed from the base shear force divided by the displacement at each incremental step, is plotted in Fig. 6b and compared against the experimental results. In general, the experimental and numerical values are very close, except for low shear strains, at which the numerical model is more flexible. It is noteworthy that the level of the applied compressive load is 3 times higher than the value of the critical bearing load according to the theory of Haringx and Gent [13,14]. However, no signs of instability were observed in the experiment. Moreover, the horizontal stiffness

increases with the horizontal displacement, also contradicting the theory of Koh and Kelly [8]. The inability of these theories to explain the behaviour of the LSF bearings may be due to the fact that they are based on a small strain assumption, i.e., they do not account for the reduction of height of the bearing subjected to vertical load, corresponding to an increased shape factor. This means that these theories assume all the geometrical parameters fixed and independent of the load, which is an accurate assumption only for high shape factors. An extension of Haringx-Gent theory to the case of small lateral deflections of rubber prisms in a prior state of homogeneous uniaxial finite strain has been derived in [10,15], where the bending and shear stiffness are expressed as functions of the axial extension ratio of the beam.

3. Shaking table tests

3.1 Prototype and test description

This subsection describes the shaking table tests carried out at the Department of Structures for Engineering and Architecture of University of Naples Federico II [6] on a prototype base-isolated building with LSF bearings. The superstructure is a one storey steel frame (Fig. 7) and it has a total height of 2900mm and plan dimensions of 2650x2150mm. The columns are fabricated by full penetration welding of four steel plates, have a box section 150x150x15mm, and they are connected to the base floor by means of a steel plate (610x450mm). The beams of the top floor are pinned to the columns and are hot-formed square hollow sections 120x120x12.5mm. The four perimetric beams at the base of the frame have HEM 160 profile.

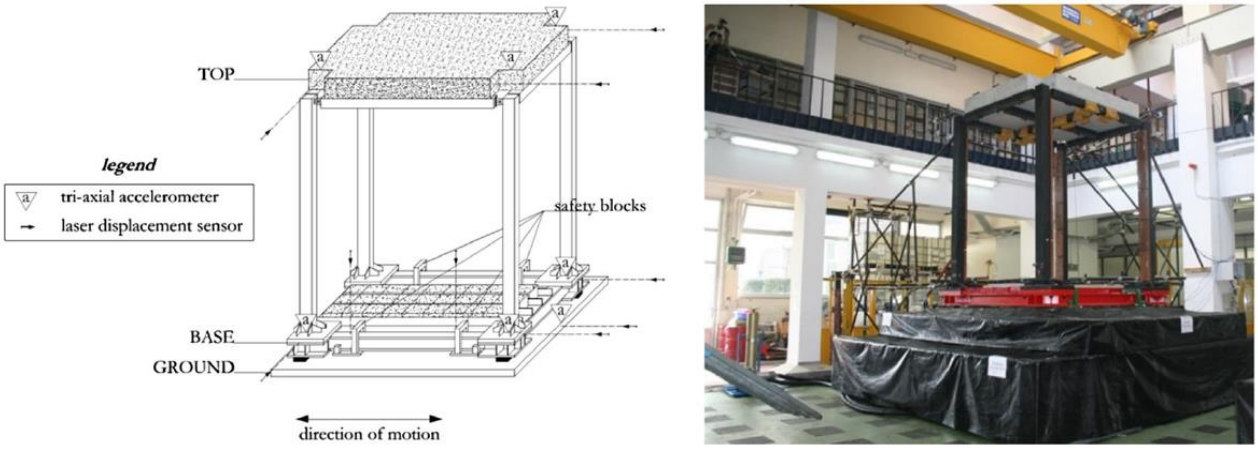

(a) (b)

Fig. 7 – (a) Cabinet projection of the prototype building and the instrumentation set-up; (b) view of the test frame of the shaking table at the DiST laboratory University of Naples Federico II [16]

Concrete blocks were added to the two levels to achieve a total mass of 7.7 tons. The total base floor mass is equivalent to 3.6 tons and the top floor mass is equal to 4.1 tons. Ground motions were applied along the direction in which the frame span is 2650 mm. The vibration period of the fixed-base structure is T_s=0.24 s. The isolation system of the scaled prototype was designed to achieve a vibration period T_{is}=0.92 s, based on an assumed value of the rubber shear modulus of 0.5MPa. It is noteworthy that the system was designed considering a geometry scale factor of 1/3 and an elastic modulus scale factor of 1. Therefore, according to the dynamic similitude rule, the equivalent period of the full-scale structure is T_{fs}= 1.59 s, (i.e. $T_{fs}= \sqrt{3}T_{is}$). A set of seven waveforms was selected from the European strong-motion database. For the scope of the present investigation, Bingol earthquake is considered, whose main characteristics are described in Table 2.

Table 2. Bingol record characteristics (Mw=, PGA=, PGV=, PGD=)

Waveform ID	Earthquake Name	Earthquake Country	Mw	Fault Mechanism	PGA (m/s²)	PGV (cm/s)	PGD (cm)
7142	Bingol	Turkey	6.3	strike slip	2.55	18.29	3.25

3.2 Numerical model

A FE model of the isolated prototype is developed to simulate the shaking table test and evaluate the behaviour of the LSF bearings under seismic excitation. Fig. 8a illustrates the developed model, which consists of only half of the total structure, due to symmetry. Beam elements (i.e. "wire elements" in Abaqus) are employed to describe the frame, whereas the same model described in the previous sections is used for the bearings. The global coordinates are defined as shown in Fig. 8, where the z axis is perpendicular to the x-y plane. The steel columns and beams of the frame are assumed to remain elastic, and thus are described by assigning a Young's modulus of 210000MPa, a Poisson's ratio of 0.3, and mass density of 7.8E-09 ton/mm^3.

Rigid elements 180mm high are used between the columns and the bearings to simulate the actual height of the beams and slab at the base floor. In the FE-model, the upper surface of the rectangular plate is connected with the bottom node of the rigid element using a "coupling kinematic connection" (see Fig. 8b). Mass elements are added to describe the bottom and top floor weight. The total weight of the superstructure model including the base beam and the top and bottom floor masses is 3.85 ton, which is half of the total superstructure mass and corresponds to a vertical load of 19kN on each rubber bearing. The out-of-plane displacement along z and rotation about x of nodes on the x-y plane are restrained to account for symmetry.

The damping property of the rubber bearings are described by using a Rayleigh damping model, whose coefficients are calculated to provide a damping ratio of 1% in correspondence of the first and second vibration modes. The coefficient α for the mass matrix and the coefficient β for the elastic initial stiffness matrix are equal to 0.067926 and 0.00080, respectively.

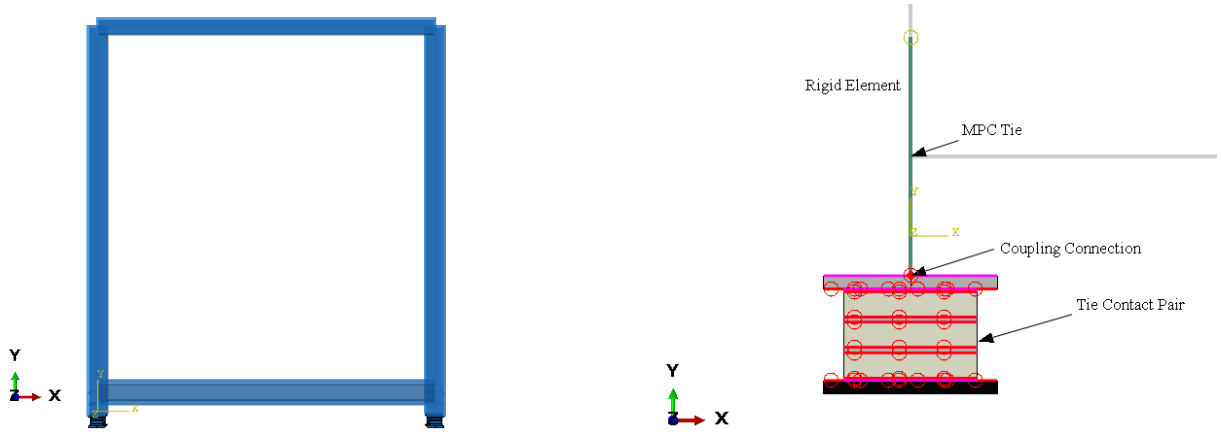

(a) (b)

Fig. 8 – (a) Finite element model of the isolated structure, (b) Contact details

Static analysis is first carried out under the self-weight of the system. Subsequently, an eigenvalue analysis is performed. The natural periods for the first two vibration modes are listed in Table 3, showing a good agreement with the experimentally values obtained from system identification of the recorded data [17]. In particular, the identification has been done taking into account the recording data from a random test

experiment that produced a peak-displacement of the bearings of 7.44 mm. The numerical model slightly overestimates the isolation period because it also slightly underestimates the bearing shear stiffness (Fig. 6b).

After application of the self-weight of the frame, dynamic implicit time-history analysis is carried out to simulate seismic response of the base-isolated frame subjected to the Bingol earthquake. Fig. 9a shows the earthquake history imposed on the bottom of the bearing in the FE analysis. The initial time step of integration is 0.02 s, which is automatically reduced, if necessary. Fig. 9b shows the time history of relative horizontal displacement of the bearing according to the experimental test [6] and the FE model. The agreement between the two responses is quite good, up to approximately 12 sec, at which point the amplitude of the input ground motion decreases and the differences between the results is more significant. This may be again due to the fact that the bearing model is more flexible than the actual bearing at low average shear strains. Fig. 10 shows the bearing deformed shape and the corresponding shear strains observed at the time when the displacement response is the highest (i.e., 48 mm). It can be observed that the local shear strains change significantly within the rubber and their values can be very different than the average one, which is 80%.

Table 3- Natural period for base-isolated model

	Natural period	
	First (Isolation mode)	Second
Numerical	1.358	0.251
Experimental	1.239	0.264

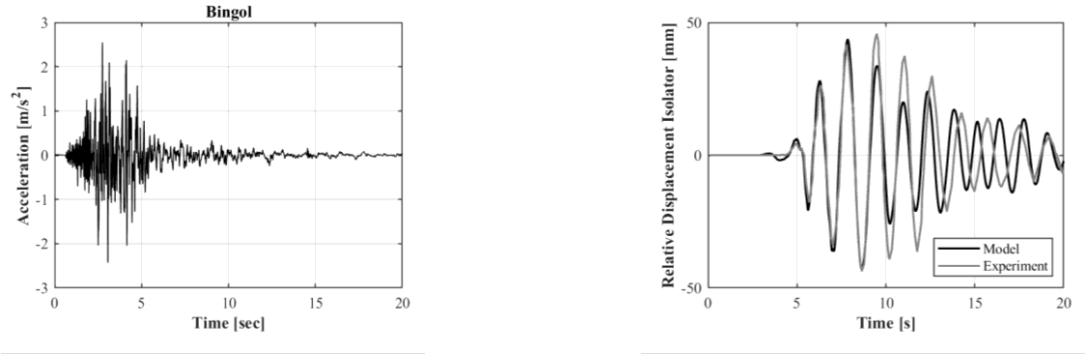

(a) (b)

Fig. 9 – (a) Input ground motion: Acceleration time history, (b) Relative Displacement Isolator time history

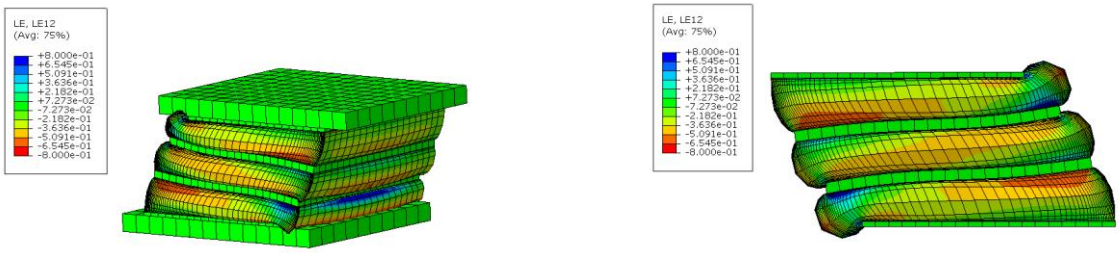

(a) (b)

Fig. 10 – Contour plot of the shear strain component within the bearing (a) 3D View, (b) Front view

4. Conclusion

This study illustrates the numerical simulation of the results of an experimental campaign carried out to characterize the behavior of structures isolated with low shape factor (LSF) bearings. Experimental tests were conducted at Tun Abdul Razak Research Center (TARRC) rubber research centre on rubber sample and LSF rubber bearings, whereas shaking table tests on a prototype of isolated structure on LSF bearings were performed at University of Naples Federico II. The numerical modeling strategy is developed in Abaqus.

The comparison between numerical and experimental results shows that the hyperelastic Ogden material model, calibrated based on the material double-shear tests, can be used to accurately describe the behavior of the unfilled natural rubber LSF bearings. In particular, the model is capable of simulating the nonlinear shear response under constant axial loading, which is characterized by significant nonlinear geometrical effects.

A numerical model of the isolated prototype tested in Naples has also been developed, by combing an advanced description of the bearings and a simplified description of the frame, using beam elements. The time history of the isolator relative displacement obtained with the model shows a quite good agreement with the experimental results.

The proposed modelling strategy is a validated tool for understanding the performance of laminated rubber bearings with low shape factor and of structures isolated with them. It allows to overcome the drawbacks of classic theories for describing the coupled vertical-horizontal behavior of laminated bearings. These theories cannot be employed for describing the behavior of LSF bearings. The proposed modelling approach can also be used for validating more advanced theories for describing the large deformation, large displacement behavior of LSF bearings.

Further validation studies will be carried out by considering additional responses measured during the shaking table tests, by also considering more advanced damping models. Moreover, the response of the prototype under both horizontal and vertical seismic inputs will be studied numerically in order to evaluate the performance of the system and the capability of the LSF bearings to provide a full three-dimensional isolation.

5. Acknowledgements

Thanks are due for support given by Prof. Giorgio Serino and Fabrizia Cilento who provided data from experimental campaign carried out at the laboratories of TARRC and Department of Structures for Engineering and Architecture of University of Naples Federico II.

6. References

[1] J. M. Kelly and D. A. Konstantinidis (2011): *Mechanics of Rubber Bearings for Seismic and Vibration Isolation.* John Wiley & Sons.

[2] M. C. Constantinou, A. Kartoum, and J. M. Kelly (1992): Analysis of compression of hollow circular elastomeric bearings. *Engineering Structures*, vol. 14, no. 2, pp. 103–111

[3] G. M. Montuori, E. Mele, G. Marrazzo, G. Brandonisio, and A. De Luca (2016): Stability issues and pressure–shear interaction in elastomeric bearings: the primary role of the secondary shape factor. *Bullettin of Earthquake Engineering*, vol. 14, no. 2, pp. 569–597.

[4] J. M. Kelly (1998): Base Isolation in Japan. *Report No. UBC/EERC-88/20*, National Science Foundation, University of California, Berkeley, USA.

[5] I. D. Aiken, J. M. Kelly, and F. F. Tajirian (1989): Mechanics of Low Shape Factor Elastomeric Seismic Isolation. *Report No. UBC/EERC-89/13*, Rockwell International Corporation, University of California, Berkley, USA.

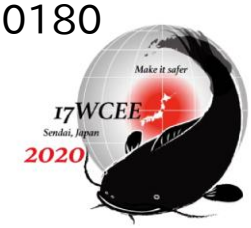

[6] F. Cilento, R. Vitale, M. Spizzuoco, G. Serino, and A. H. Muhr (2017): Analysis of the Experimental Behaviour of Low Shape Factor Isolation Rubber Bearings by Shaking Table Investigation. *17th Convegno L'ingegneria Sismica in Italia, ANIDIS XVII, Pistoia, Italy.*

[7] G. P. Warn and B. Vu (2012): Exploring the low shape factor concept to achieve threedimensional seismic isolation. *20th Analysis and Computation Specially Conference*, no. 1, pp. 1–11.

[8] C. G. Koh and J. M. Kelly (1989): Modelling of seismic isolation bearings including shear deformation and stability effects. *Applied Mechanics Reviews*, vol. 42, no. 11, pp. 113–120.

[9] C. G. Koh and J. M. Kelly (1988): A simple mechanical model for elastomeric bearings used in base isolation *International Journal of Mechanical Science*, vol. 30, no. 12, pp. 933–943.

[10] A. H. Muhr (2017): Lateral stiffness of rubber mounts under finite axial deformation. *Constitutive Model for Rubber X - Proceeding of the European Conference on Constitutive Model for Rubber, ECCMR X*, pp. 153–158.

[11] "Dassault Systèmes, Abaqus Analysis User's Manual Version 2018."

[12] K. N. Kalfas, S. A. Mitoulis, and K. Katakalos (2017): Numerical study on the response of steel-laminated elastomeric bearings subjected to variable axial loads and development of local tensile stresses. *Engineering Structures* , vol. 134, pp. 346–357.

[13] J. A. Haringx (1949): Elastic Stability of Helical Springs At a Compression Larger Than Original Length. *Flow, Turbulence and Combustion.* pp. 417–434.

[14] A. N. Gent (1965): Elastic Stability of Rubber Compression Springs. *Rubber Chemistry and Technology*, vol. 38, no. 2, pp. 415–430.

[15] I. R. Goodchild, A. H. Muhr, and A. G. Thomas (2018): The lateral stiffness and damping of a stretched rubber beam. *Plastic Rubber and Composites*, vol. 47, no. 4, pp. 176–186.

[16] A. Calabrese, M. Spizzuoco, G. Serino, G. Della Corte, and G. Maddaloni (2015): Shaking table investigation of a novel, low-cost, base isolation technology using recycled rubber. *Structural Control and Health Monitoring*, no. 22, p. 107-122.

[17] P. Van Overschee and B. De Moor (2008): *Subspace Identification For Linear Systems*, Kulwer Academic Publishers.

